To Appear in the IEEE Transactions on Signal Processing

A New Flexible Bi-orthogonal Filter Design for Multiresolution Filterbanks with Application to Image Compression *

Nikolay Polyak† and William A. Pearlman‡

Electrical, Computer and Systems Engineering Department

Rensselaer Polytechnic Institute, Troy, NY, 12180-3590

E-mail: pearlman@ecse.rpi.edu

Phone : (518) 276-6082, Fax: (518) 276-6261

February 18, 2000

Abstract

In this article we propose a new fast method with great potential for multiresolution pyramid decomposition of signals and images. The method allows unusual flexibility in choosing a filter for any task involving the multiresolution analysis and synthesis. Using our method, one can choose any low pass filter for the multiresolution filtering. This method enabled us to choose the best filters for SPIHT image compression for the corresponding support sizes. The compression results for our 7 tap filters are better than those of the 9/7 wavelet filters and approximately the same as those of the 10/18 filters, while at the same time our 7 tap filters are faster than 10/18 filters.

EDICS SP 2.4.4

*This material is based upon work suppoorted by the National Science Foundation under Grant No. NCR-9004758. The government has certain rights in this material.

†Currently with Thomson Financial Services, E-mail nick.polyak@tfn.com

‡Corresponding author

1 Introduction

1.1 Filter Banks

The filter bank depicted in Figure 1 decomposes an input signal into several channels and downsamples the output of each channel on the decomposition side. After the decomposition, some processing, e.g. compression, is usually done. Finally on the reconstruction side, the channels are upsampled by inserting zeros between neighboring samples, passed through the reconstruction filters and summed. The filter banks, are called perfect reconstruction filter banks if they reconstruct perfectly the input signal at the output when processing is omitted between the downsampling in the decomposition and the upsampling in the reconstruction.

The theory of the filter banks was developed in many previous works (e.g. [17], [18], [19], [10], [6], [24], [22], [23], [21]). Here we present a new methodology allowing more flexibility in choosing perfect reconstruction filter banks.

1.2 Wavelet Decomposition

Wavelet transform applied to signal and image processing results in a recursive filtering algorithm, in which a signal is decomposed into low and high bands using the low and high pass filters and subsampled by a factor of 2. The low band is then recursively decomposed in the same manner. In the reconstruction stage, we start from the two lowest bands, upsampling them, passing them separately through the low and high pass reconstruction filters and summing their outputs. Then take this sum and the next lowest band as the second band and repeat the procedure, until the whole signal is reconstructed. In each decomposition stage the two channel decomposition filter bank is applied to the input signal and on each reconstruction stage the two channel reconstruction filter bank is applied to the high and low decomposition bands. In order for the output signal to be the exact copy of the input, the decomposition and reconstruction filter bank should constitute a perfect reconstruction pair.

Images are split initially into four subbands by applying low and high pass filters followed by factor of two downsampling separably in each of the two dimensions, thereby splitting them into

high-high, high-low, low-high and low-low horizontal-vertical spatial frequency subbands. Emulating the procedure for one dimension, the same low and high pass filtering is then applied repeatedly to the low-low subband. In reconstruction, the process is reversed by upsampling each of the four subbands at the coarsest scale by two and filtering with the appropriate filter in each dimension, summing the four filtered subbands to produce the low-low subband at the next finer scale, and repeating until the full scale reconstructed image is reached.

A diagram depicting the wavelet subbands of an image to two levels of decomposition is shown on Figure 2. This type of a recursive decomposition was shown to concentrate most of the signal energy in the low bands, which is good for compression purposes. The earliest major published work that used a subband decomposition for compression of images is attributed to Woods and O'Neil [7]. The theory of wavelet decomposition has been recently advanced by Daubechies in [4] and [11] and by Mallat for two dimensions in [1], [2], and [3], with further expositions by Cohen [9] and Vetterli [10] and co-workers among others.

1.3 Filter Banks for Wavelet Decomposition

The central problem in a wavelet transform is choosing the two filter decomposition and reconstruction filter banks. At first research concentrated on the orthogonal wavelets, resulting in strict Quadrature Mirror Filter (QMF) conditions on the perfect reconstruction filter banks. Such FIR (finite impulse response) filters found in [1] or [4] are shown to have either large support or not very good compression properties. If the perfect reconstruction property is relaxed, the QMF conditions are not as restrictive and might result in better filters, e.g., see [8]. The QMF conditions combined with the perfect reconstruction, lead to the requirement that all the shifts by a multiple of two (2-shifts) of the impulse responses of the low and high pass filters of the filter bank taken together would form an orthogonal basis in the space of all square summable discrete sequences l_2. In such a case, the reconstruction filter bank is the same as the decomposition one.

Because of these problems with the orthogonal filter, the biorthogonal approach was tried in [9], [10], [11], [13], and other works, but only FIR solutions were found. In [6] only orthogonal IIR filters were considered in a solution to the perfect reconstruction problem, and resulted in large

support filters.

In [23] based on theory developed in [24] infinite impulse response (IIR) linear phase filters were constructed. These filters can be considered predecessors to the filters obtained here. There are important differences though. Our theoretical results are more general and our practical results are much better. Based on theory in [24], one can derive linear phase filters only with even support size. We show how to find such filters for any support size. The only condition for our filter bank to have the perfect reconstruction property, would be orthogonality of the filters in different subbands, while in [24] for linear phase filters a stricter mirror condition is imposed. The decomposition and reconstruction filters in [23] and [24] are not quite linear phase because they perform the recursive causal filtering in decomposition and anticausal filtering in reconstruction stages. That makes their impulse responses non-symmetric with respect to any vertical line, which is necessary for linear phase. We perform both causal and anticausal filtering either in the decomposition or reconstruction stage thus ensuring that our filters are linear phase. Giving up on linear phase property causes computational inefficiencies with symmetic extension of finite images, so that it is necessary to resort to periodic extension. This might lead to discontinuities on edges and poorer compression performance.

1.4 Organization of the Paper

In Section 2 we present the main theory and give an example of finding a perfect reconstruction filter bank. In Section 3 the best filters for several support sizes are found and simulation results are presented. Summary and conclusions are given in Section 4.

2 Theory of Orthogonal Subband Perfect Reconstruction Filter Banks

2.1 Background on the Zak Transform

The Zak theory for signal processing was developed in [20], [16], [15] and [21]. The Zak transform has the same relation to the polyphase representation (see [17], [18], [19]) as the Fourier transform to the Z-transform. In [21] we showed that the Zak transform is very suitable for treating the filter bank theory without having exceptions for undersampling and unstable cases. By undersampling we mean a case when the decimation factor is larger than the number of channels in the filter bank. We applied the Zak transform theory to obtain new results in the theory of filter banks. Some of these results, needed for the proof of the main theorem of this paper, are given here without proofs. Their proofs can be found in [21].

Definition 1 *Let $g[k]$ be function from l_2. The discrete M-Zak transform of the function $g[k]$ is*

$$Z_M(g)(\omega, m) = \sum_{i=-\infty}^{\infty} g[m + iM]e^{-j2\pi\omega i}, \tag{1}$$

$$-\pi \geq \omega \geq \pi, 0 \leq m < M - 1. \tag{2}$$

Theorem 1 *Let $s[k]$, an l_2 signal be the input to a filter $h[k]$. The output after decimation by M is*

$$c[l] = \sum_{k=-\infty}^{\infty} h[k]s[Ml - k] = \sum_{k=-\infty}^{\infty} h[Ml - k]s[k], \tag{3}$$

for any integer l. Then

$$c[l] = \frac{1}{2\pi}\int_{\omega=-\pi}^{\pi}(\sum_{m=0}^{M-1} Z_M(h)(\omega, m)Z_M(s)(\omega, -m))e^{j2\pi\omega l}d\omega. \tag{4}$$

By taking the Fourier transform of both parts of the equation, we obtain the formula for the Fourier transform of the M-decimated filtering coefficients. Denoting it by $C_M(\omega)$, we have:

$$C_M(\omega) = \sum_{m=0}^{M-1}(Z_M(h)(\omega, m)Z_M(s)(\omega, -m)). \tag{5}$$

Theorem 2 *Suppose we have a one channel reconstruction filter bank, consisting of an M-interpolator and a filter as shown on Figure 3. We can find a one channel decomposition filter bank, consisting*

of a decomposition filter and an M-decimator as shown on Figure 4, which minimizes the sum of the squared differences between the output and input signals. Denoting the impulse response of the reconstruction filter by h we can find the impulse response of the optimal decomposition filter $\tilde{h}$ through the following formula:

$$\tilde{h}[m+iM] = \frac{1}{2\pi}\int_{\omega=-\pi, H_M(\omega)\neq 0}^{\pi} \frac{Z_M(h)(\omega,m)}{H_M(\omega)} e^{j2\pi\omega i} d\omega, \tag{6}$$

where $0 \leq m < M$, i any integer and

$$H_M(\omega) = \sum_{r=0}^{M-1} |Z_M(h)(\omega,r)|^2. \tag{7}$$

The filter impulse response $\tilde{h}$ is the inverse M-Zak transform of $\frac{Z_M(h)(\omega,m)}{H_M(\omega)}$. Notice that

$$Z_M(\tilde{h})(\omega,m) = \begin{cases} \frac{Z_M(h)(\omega,m)}{H_M[n]}. & \text{if } H_M(\omega) \neq 0 \\ 0 & \text{if } H_M(\omega) = 0 \end{cases} \tag{8}$$

Definition 2 *We call the optimal decomposition filter as the one of Theorem (2), biorthogonal to the reconstruction filter. One can see that the biorthogonality property is mutual: the filter biorthogonal to the optimal decomposition filter would be the original reconstruction filter*

Definition 3 *In case we have two decomposition or reconstruction subband channels or filters, each one as shown in Figure 4 and Figure 3, with M-decimation or interpolation, we call them mutually orthogonal, if all the M-shifts of the first channel filter impulse response functions span a subspace of l_2 orthogonal to the span of all M-shifts of the second channel filter impulse response functions.*

Notice that the orthogonality of filters is a much less strict condition than the full wavelet orthogonality, since the M-shifts of each filter impulse response functions are not required to be orthogonal between themselves.

Theorem 3 *The M-shifts of the biorthogonal filters impulse response functions span the same subspace of l_2.*

Theorem 4 *Having several mutually orthogonal reconstruction filters, we can use their respective biorthogonal filters for the corresponding decomposition channels to obtain the best reconstruction in the minimum squared error sense of the input signal on the output.*

Theorem 5 *Having M mutually orthogonal reconstruction filters for the M-decimation-interpolation scheme, and using their respective biorthogonal filters for the decomposition we obtain a perfect reconstruction filter bank if the M-shifts of all of the reconstruction filters impulse response functions taken together span all of l_2.*

The last condition for the M-shifts of M orthogonal filter banks to span the whole l_2 is not a very strict condition. It holds for the filter banks with finite support and good concentration of energy properties. Below, we omit this condition from our discussions.

2.2 The Main Result

The novelty of our approach lies in the fact that on one hand we consider the orthogonal filters wavelet transform and do not restrict ourselves to FIR filters as did many wavelet researchers. Instead we look for recursive biorthogonal filters. Switching to the recursive filters gives us additional degrees of freedom, thus enabling us to drop the restrictive conditions imposed on the filter banks because of the FIR requirement and find filters with virtually arbitrary impulse response. On the other hand we extensively use the orthogonality of subband channels and look for individual filter optimal solutions in order to find the globally optimal solution, which cannot be successfully handled by the polyphase representation theory.

Definition 4 *The M-phase representation of a discrete function $f[n]$ is given by M functions: $\mathcal{F}_0(z), \mathcal{F}_1(z), \ldots, \mathcal{F}_{M-1}(z)$, where*

$$\mathcal{F}_i(z) = \sum_k g[i + kM] z^k. \tag{9}$$

One can see, that

$$\mathcal{F}_i(e^{-j\omega}) = Z_M(f)(\omega, i), \tag{10}$$

where Z_M if the M point Zak transform for the infinite signals as in (1). For the properties of the polyphase representation one can see [17], [10], and [19].

Definition 5 *For any filter f and its shift by Mn samples, f_{Mn}, let us call their inner product function*

$$A_M(f)[n] = < f, f_{Mn} >, \tag{11}$$

its M-shift autocorrelation function and its 2 sided Z-transform,

$$A_M(f)(z) = \sum_{n=-\infty}^{\infty} A_M(f)[n] z^{-n}, \tag{12}$$

its M-shift moment generating function.

Then we have the following theorem:

Theorem 6 *Suppose that we have M discrete l_2 filters $h^{(0)}, \ldots, h^{(M-1)}$ (here the superscript is not a scale as in the previous section), whose M-shifts span M mutually orthogonal subspaces of l_2 and which taken all together span the whole l_2, as a decomposition filter bank. Suppose also that $\mathcal{H}_i^{(k)}(z)$ is their M-phase representations. We obtain perfect reconstruction, by taking the reconstruction filters $\tilde{\mathcal{H}}^{(0)}, \ldots, \tilde{\mathcal{H}}^{(M-1)}$ with the following M-phase representation:*

$$\tilde{\mathcal{H}}_i^{(k)}(z) = \frac{\mathcal{H}_i^{(k)}(z)}{A_M(h^{(k)})(z)}, \tag{13}$$

where $i, k = 0, 1, \ldots, M-1$ and $A(h^{(k)})(z)$ is the M-shift moment generating functions of the filter $h^{(k)}$.

The proof of the theorem is given in the next subsection.

By taking a particular case of this theorem with $M = 2$, arbitrary low pass filter h and high pass filter g being the mirror of h, given by the formula

$$g[i] = (-1)^{i+1} h[1-i], \tag{14}$$

we can apply the theorem to the orthogonal filters wavelet transform. Indeed as was stated in the previous section, the even shifts of h and g constitute orthogonal subspaces of l_2 because of the mirror property. The only concern is that the even shifts of both functions taken together span the whole l_2 space, but most of the discrete l_2 functions satisfy this property. The resulting reconstruction filters have the following 2-phase representation:

$$\tilde{\mathcal{H}}(z) = \frac{\mathcal{H}(z)}{A_2(h)(z)} \tag{15}$$

$$\tilde{\mathcal{G}}(z) = \frac{\mathcal{G}(z)}{A_2(g)(z)}. \tag{16}$$

Notice that dropping the FIR requirement allowed us to use the mirror filter g for the decomposition as a high-pass filter. In [9], [11] and [10] it was used for reconstruction and therefore could not be used for decomposition.

The theorem gives us several ways to do decomposition and reconstruction.

We can take h to be any low pass filter and then take g to be its mirror filter as in (14). We decompose the source signal by applying these filters and decimating by 2. Then, we apply the filters r_h and r_g whose Z-transforms are given by $R_h(z) = 1/A_2(h)(z)$, $R_g(z) = 1/A_2(g)(z)$ to the corresponding subbands, 2-interpolate the coefficients in both subbands, pass them through the filters h and g and sum the results. Note that because of the mirror property $A_2(h)(z) = A_2(g)(z)$ and therefore the IIR subband filters are the same in both subbands: $r_h = r_g$. We shall refer to $A_2(h)(z)$ and $A_2(g)(z)$ as $A_2(z)$ and to the filters r_h and r_g as r. We call r the auxiliary IIR (infinite impulse response) filter. Filter r can be implemented as a recursive filter. Because the polynomial A_2 is even (it is a Z-transform of a 2-decimated autocorrelation function), the filter whose Z-transform is $A_2(z)$ is not stable (for every root at x of the filter, there is also a root at $1/x$). In order to implement such a filter, we create another filter by grouping together all the roots of $A_2(z)$ whose absolute value is smaller than one. During the filtering we go through the following steps. First we filter the signal with with this filter, and then reverse the output signal in time and apply it to a second identical filter. The desired result is the time-reversed output of this second filtering step.

The factor $1/A_2(z)$ can be absorbed into the decomposition, which is equivalent to exchanging the decomposition and reconstruction filters and taking $\tilde{h}$ and $\tilde{g}$ to be the decomposition filters, while using h and g for reconstruction. Compression in this case is performed after the recursive filtering. These considerations lead us to the filter bank diagram presented in Figure 5.

2.3 Proof of the Main Result

We assume the notations of Theorem (6). The fact that the M-shifts of $h^{(0)}, \ldots, h^{(M-1)}$ span M mutually orthogonal subspaces $H^{(0)}, \ldots, H^{(M-1)}$ and together span the whole l_2 allows us use of Theorem (5). In other words by finding the individual biorthogonal filters to all of the filters

from the original set and using the original filters for reconstruction and the biorthogonal ones for decomposition or the other way around, we obtain a perfect reconstruction filter bank.

We use Theorem (2) and equation (8) for finding the Zak Transform of the reconstruction filters, which, because of the orthogonality of the subspaces are the filters individually biorthogonal to each of the filters of the set in the sense of the theorem. From (8) one can see that the M-Zak transform (an equivalent of the M-phase representation) of the biorthogonal filters (assuming $H_M^{(i)}(\omega) \neq 0$) is given by

$$Z_M(\tilde{h}^{(i)})(\omega, m) = \frac{Z_M(h)(\omega, m)}{H_M^{(i)}(\omega)}. \tag{17}$$

Using equation (7) and the fact that

$$\bar{Z}_M(h)(\omega, m) = Z_M(h)(\omega, -m), \tag{18}$$

we derive that

$$H_M^{(i)} = \sum_{r=0}^{M-1} Z_M(h^{(i)})(\omega, r) Z_M(h^{(i)})(\omega, -r) \tag{19}$$

Now looking at equation (5), we observe that $H_M^{(i)}$ is the Fourier transform of the M decimated result of the filtering of a signal $h^{(i)}$ with the filter of the same impulse response $h^{(i)}$. Switching from the Fourier transform to the Z-transform and from the Zak Transform to the polyphase representation, we obtain (13).

2.4 An Example of Computing a Filter

As an example we illustrate the construction with the following low pass analysis filter coefficients:

$$h[-1] = 0.5, h[0] = 1, h[1] = 0.5, \tag{20}$$

and all the remaining coefficients of h are zero. The corresponding non-zero high pass filter ceffi-cients are found according to (14):

$$g[0] = -0.5, g[1] = 1, g[2] = -0.5. \tag{21}$$

The even-shift moment generating function is

$$A_2(z) = (z^{-1} + 6 + z)/4. \tag{22}$$

Correspondingly, the auxiliary IIR filter has the following Z-transform:

$$R(z) = \frac{4}{z^{-1} + 6 + z}. \tag{23}$$

Factoring the denominator, we obtain

$$R(z) = \frac{4(\sqrt{2}-1)^2}{(z^{-1} + (\sqrt{2}-1)^2)(z + (\sqrt{2}-1)^2)}. \tag{24}$$

Another useful form is obtained from the partial fraction expansion

$$R(z) = \frac{1}{\sqrt{2}}\left(\frac{1}{(z^{-1} + (\sqrt{2}-1)^2)} + \frac{1}{(z + (\sqrt{2}-1)^2)} - 1\right). \tag{25}$$

Using the form of (24), we factor out the stable part of the filter, creating the filter r' with the Z-transform:

$$R'(z) = \frac{2(\sqrt{2}-1)}{(z^{-1} + (\sqrt{2}-1)^2)}. \tag{26}$$

We pass the input through this recursive filter, and then pass the time-reversed output through the same filter. The time-reversal of the latter output yields the final result.

According to the form of (25), we use the filter r'':

$$R''(z) = \frac{1}{(z^{-1} + (\sqrt{2}-1)^2)} = \frac{R'(z)}{2(\sqrt{2}-1)}. \tag{27}$$

We pass both the signal and its time-reversal separately through the filter, sum the two outputs, and subtract the original signal from the sum. Finally we multiply the result by $\frac{1}{\sqrt{2}}$.

3 Finding the Best Filters for a Given Support, Simulation Results

3.1 Implementation and Choosing the Best Filter

The recursive post filtering ($\frac{1}{A(g)(z)}$ factor in equations (15) and (16)) can be performed either in the decomposition or the reconstruction stages. In all cases, partial fraction expansion was employed as in equations (25) to (27) to actuate the filtering. As a result of numerous experiments in which images were compressed using different filters, it was noticed that the best compression results are obtained when the recursive filtering is done in the decomposition stage for the low bands and in the reconstruction stage for the high bands as shown in Figure 6. Some further research is necessary to understand why this happens.

The SPIHT compression algorithm [14] was run on image wavelet subbands, produced by separable filtering with different filters and supports up to 7 for decomposition and reconstruction, inserting the appropriate recursive auxiliary filter in each dimension at each stage.

In application to compression the low-pass filters were normalized to have their sum equal $\sqrt{2}$. Their mirror filters were used as the high-pass filters.

In [27], [28], [29] and other publications different methods for choosing the optimal filters are described. All of them, however are dealing with orthogonal filtering and compression algorithms different from SPIHT. Because of that the filters that produce the best results for Lena image and 0.25 bpp rate were found by a trial and error procedure. Since these results turned out to be good also for other rates on Lena and Barbara images, we think that the algorithm should provide good compression results for a wide spectrum or rates and images.

The resulting unnormalized tap values of the low pass filters were as follows:

[1 2 1] for support 3,

[-1 2 10 10 2 -1] for support 6,

and

[-1.047 -0.347 6 10.6 6 -0.347 -1.047] for support 7.

An integer filter [-1 -0.5 6 11 6 -0.5 -1] with support size 7 also proved to produce good results (see

[5]), but here we report slightly better results with the latter floating point support size 7 filter.

During the search procedure we tried all the possible combinations of the filter tap values with the linear phase restriction on the filters. The change step for each of the taps was 0.5. In case of the 7 tap filter we ran the algorithm several times, reducing the step size in order to improve the results. The lowest and highest bounds on the changes were chosen to be large enough that all the reasonable filters would fall between them.

The results for supports 4 and 5 were worse than those for the support 3 and are not produced here. This corroborates the conclusions of [25] made for filters corresponding to an orthogonal wavelet transform, that increasing the number of taps does not necessarily lead to the performance improvement.

3.2 Compression Results

The simulations were conducted by transforming and compressing 512 by 512 Lena and Barbara monochrome images. The SPIHT compression algorithm without the subsequent entropy coding was used (see [14]). Our 3, 6, and 7 tap filters, the 9/7 (see [13]), the 10/18 filters (see [12]), and two filters denoted A1 and A2 (see [23]) were tested and compared in performance in SPIHT compression for these two images at several rates. The 9/7 and 10/18 are considered to be among the best practical FIR filters for compression and the A1 and A2 filters are considered to be the best IIR filters. The results are summarized in Table 1, where the entries for each rate in bits per pixel and filter type is peak signal-to-noise ratio in dB (PSNR), defined as

$$PSNR = 10 \log_{10}(\frac{255^2}{MSE}) dB, \tag{28}$$

where MSE is the mean squared error.

We used the filters from [23] differently from the way they were used there. There in order to utilize the all pass property of the filters, which allows fast implementation, the causal recursive filtering was performed on the decomposition stage, while the anticausal on the reconstruction stage. This means giving up on the linear phase property of the filters. Here, however, we use the procedure similar to what we use for our filters, performing all of the recursive filtering on the decomposition stage for the low bands and on the reconstruction stage for the high bands. Another

distinction is that the in [23] a decomposition results in the number of the coefficients greater than the number of pixels in the original image while in our case, the number of the coefficients is the same. Finally in [23] a different compression algorithm was employed. In order to compare the filters, we took the filters from [23] and used them in the same way as we used our filters. The filters from [23] thus become the 4 and 8 tap linear phase filters presented below:
[1 3 3 1],
[0.0437 -0.1000 0.4827 1.000 1.000 0.4827 -0.1000 0.0437]. In Table 1 we denote them by A1 and A2. Figures 7 and 8 contain the plots of the results.

The simulation results show the steady superiority of our 7 tap filter and 10/18 filter from [12] over all the other filters. Next in line is the 9/7 filter of [13] followed by the 6 and 3 tap filters. The filters from [23] are at the end of the performance hierarchy and the smaller filter performs better than the longer one.

We also show the pictures of the restored images compressed at 0.25 bpp rate for the best filters in Figure 9 for Lena and Figure 11 for Barbara. The details in the hat for Lena and the texture on the piece of clothes hanging from the table for Barbara images are better reproduced in the case of our 7 tap filter with recursive post filter, than with the 9/7 filter result.

3.3 Complexity Computation and Comparisons

In our simulations we used the algorithm based on the method of equation (25) and here we calculate the complexity for this case.

Let us denote the number of the required summations by S, multiplications by P, the number of filter taps by T. The complexity in general case can be computed as the number of the required floating point operations per sample of a one dimensional signal, per scale. On the original scale the number of floating point operations per pixel for the algorithm proposed in this paper, during both the decomposition and reconstruction is given by the following formulas:

$$P = 2T + 2\lfloor\frac{T-1}{2}\rfloor \tag{29}$$

$$S = 2T - 2 + 2\lfloor\frac{T-1}{2}\rfloor. \tag{30}$$

Comparison of Compression Results for Lena Image							
rate (bpp)	*3 Tap*	*6 Tap*	*7 Tap*	*9/7*	*10/18*	*A1*	*A2*
0.15	30.93	31.43	31.58	31.48	31.64	30.58	29.33
0.2	32.19	32.61	32.83	32.72	32.82	31.88	30.26
0.25	33.10	33.56	33.84	33.70	33.84	32.90	31.28
0.3	33.85	34.38	34.68	34.53	34.65	33.54	31.93
0.35	34.57	35.16	35.27	35.17	35.42	34.29	32.27
0.4	35.32	35.69	35.92	35.83	35.93	34.99	32.86
0.45	35.77	36.22	36.47	36.38	36.44	35.64	33.42
0.5	36.20	36.72	36.94	36.85	36.93	35.87	34.03
Comparison of Compression Results for Barbara Image							
rate (bpp)	*3 Tap*	*6 Tap*	*7 Tap*	*9/7*	*10/18*	*A1*	*A2*
0.15	25.20	25.54	25.64	25.66	25.57	24.36	23.82
0.2	26.29	26.72	26.87	26.69	26.91	25.13	24.43
0.25	26.95	27.70	27.87	27.72	27.91	26.13	25.01
0.3	27.79	28.42	28.84	28.68	28.75	26.73	26.09
0.35	28.64	29.48	29.81	29.58	29.82	27.67	26.62
0.4	29.55	30.28	30.64	30.33	30.72	28.88	27.73
0.45	30.21	30.82	31.26	30.93	31.30	29.94	28.59
0.5	30.66	31.44	31.98	31.63	32.01	30.48	29.40

Table 1: PSNR (dB) versus rate of compression for several filter types

In case of the biorthogonal filters with sizes $T1$ and $T2$, the formulas are

$$P = T1 + T2 \tag{31}$$

$$S = T1 + T2 - 2. \tag{32}$$

In all of the special cases considered above, however all of the filters are either symmetric or antisymmetric. For that case, we have:

$$P = 2\lfloor \frac{T+1}{2} + 2\lfloor \frac{T-1}{2} \rfloor \tag{33}$$

$$S = 2T - 2 + 2\lfloor \frac{T-1}{2} \rfloor \tag{34}$$

for the algorithm proposed in this paper. For the biorthogonal filter algorithm we have:

$$P = \lfloor \frac{T1+1}{2} \rfloor + \lfloor \frac{T2+1}{2} \rfloor \tag{35}$$

$$S = T1 + T2 - 2. \tag{36}$$

For every subsequent scale the number of both multiplications and additions of the previous scale should be divided by 2.

For two dimensional signals (images), with separable filtering, we need to multiply the above formulas by 2 (to account for horizontal and vertical filtering) and for each subsequent scale, we divide the number of the operations by 4, since the number of pixels on each scale is 4 times smaller than that of the previous one. Now using the equations (33), (34), (35) and (36) we can compare the complexity for all of the methods involved.

Ansari et al filters in [23], were actually implemented faster than the filters A1 and A2 from the table 2. This is due to the all pass property of the filters which allows to utilize the symmetricity of the recursive and non-recursive part of the filters. For the full description of the all pass property we refer to [23]. However as was mentioned above, in that case, the linear phase property of the filters is lost and the finite signal or image needs to be periodically extended, which might cause loss of continuity at the image borders.

It can be seen that the complexity of our 7 tap filter exceeds that of the 9/7 filter by the factor of 1.39, while the complexity of the the 10/18 filter exceeds the complexity of our filter by the factor of 1.25.

Complexity Comparison							
operation	*3 Tap*	*6 Tap*	*7 Tap*	*9/7*	*10/18*	*A1*	*A2*
multiplications	6	10	14	9	14	6	14
summations	6	14	18	14	26	8	20
overall	12	24	32	23	40	14	34

Table 2: Complexity comparison in operations per pixel on the largest scale.

4 Summary and Conclusions

In this paper we presented a new, fast and very promising method of performing the wavelet transform and reconstruction. The method allows an unusual flexibility in choosing the wavelet filters. One can choose almost any filter to be the low-pass filter of the filter pair and the high pass filter would be its mirror filter. The reconstruction is performed using the same filter pair. In order for the scheme to have a perfect reconstruction property, short recursive filtering is inserted between for the decomposed signal.

Assuming the infinite impulse response for the wavelet filters was shown to increase the flexibility in choosing the wavelet transform ([22], [24] and [6]). Our method, however, results in more comprehensive choice options and faster performance than methods presented previously. Indeed, the theory developed in [24] results only in even support size linear phase mirror filters for two channel filter banks, while our method achieves a perfect reconstruction M channel filter bank for any support size, with the looser subband orthogonality property instead of the mirror property. Also while in [23] and [24], it was proposed to have causal recursive filter on the decomposition stage and anticausal on the reconstruction stage, we perform all of the recursive filtering on one of the stages, thus preserving the linear phase property of the filters. The SPIHT compression results with our filters are are much better than those with the filters from [23]. Furthermore, in [6] only orthogonal IIR filters are considered, which results in large support filters.

As a result of the flexibility of our method, we are able to choose the best filter pair for a given support size by conducting the experiments. As a result of the experiments, the best filters for the support sizes 3, 6 and 7 were found. The results for supports 4 and 5 were worse than those for the support 3 which corroborates the conclusions of [25] made for filters corresponding to an orthogonal wavelet transform, that increasing the number of taps does not necessarily lead to the performance improvement. The renowned 9/7 filter pair of [13] is slightly better than our 6-tap filter in performance and complexity. However, the compression results for our 7 tap filter are better than those of the 9/7 filters and approximately the same as those of the 10/18 filters of [12], considered to be among the best filters. Regarding speed to perform analysi and synthesis, the 7 tap filter is slower than the 9/7 filters, but faster than the 10/18 filters.

Our method allows a new degree of freedom for choosing the wavelet filters. Using it one can customize the filters according to the application. We did this for image compression. Some other uses can be considered, such as multiplexing and noise reduction.

References

[1] S. Mallat, "A Theory for Multiresolution Signal Decomposition: The Wavelet Representation," *IEEE Trans. on Patt. Anal. Mach. Intell.*, vol. 11, no. 7, pp. 674–693, July 1989

[2] S. Mallat, "Multiresolution Approximation and Wavelet Orthonormal Bases of L^2," *Am. Math. Soc.*, vol. 315, pp. 69-88, 1989

[3] S. Mallat, "Multifrequency Channel Decomposition of Images and Wavelet Models," em IEEE Trans. on Acoustics, Speech and Signal Processing, vol. 33, no. 12, pp. 2091-2110, Dec. 1987

[4] I. Daubechies, "Orthonormal Basis of Compactly Supported Wavelets," *Comm. Pure Applied Math.*, vol. 41, pp. 909-996, 1988

[5] N. Polyak, W. A. Pearlman, "Wavelet Decomposition and Reconstruction Using Arbitrary Kernels: A New Approach", *Proc. IEEE 1997 Internation Conference on Image Processing*, Santa Barbara, CA, Vol. 1, pp. 660-663, Oct. 1997

[6] C. Herley, M. Vetterli, "Wavelets and Recursive Filter Banks", *IEEE Trans. on Signal Processing*, vol. 41, pp. 2536-2556, Aug. 1993

[7] John W. Woods, Sean D. O'Neil, "Subband Coding of Images", *IEEE Trans. Acoustics, Speech and Signal Processing*, ASSP-35(5), pp. 1278-1288, Oct. 1986

[8] J. D. Johnston, "A Filter Family Designed for Use in Quadrature Mirror Filter Banks", *Proceedings IEEE International Conf. on Acoust. Speech and Signal Processing*, ICASSP-1980, pp. 291-294, 1980.

[9] A. Cohen, I. Daubechies and J.-C. Feauveau "Biorthogonal Bases of Compactly Supported Wavelets", *Communications on Pure and Applied Math.*, vol. XLV, pp. 485–560, 1992.

[10] M. Vetterli, C. Herley "Wavelets and filter banks: Theory and Design", *IEEE Trans. on Signal Processing*, vol. 40, pp. 2207-2232, Sept. 1992.

[11] I. Daubechies, "Ten Lectures on Wavelets", Society for Industrial and Applied Mathematics, 1992

[12] M. J. Tsai, J. D. Villasenor, F. Chen, "Stack-Run Image Coding", *IEEE Trans. on Circuits and Systems for Video Technology*, Vol. 6, pp. 519-521, Oct. 1996

[13] M. Antonini, M. Barlaud, P. Mathieu, I. Daubechies, "Image Coding Using Wavelet Transform", *IEEE Trans. on Image Processing*, vol. 1, No. 2, pp. 205-220, April 1992

[14] A. Said, W. A. Pearlman, "A New Fast and Efficient Image Codec Based on Set Partitioning in Hierarchical Trees",*IEEE Trans. on Circuits and Systems for Video Technology*, vol. 6, pp. 243-250, June 1996.

[15] Auslander, L., Gertner, I. C., Tolmieri, R., "The Discrete Zak Transform Application to Time-Frequency Analysis and Synthesis of Nonstationary Signals",*IEEE Trans. on Signal Processing*, Vol. 39, No. 4, Apr. 1991, pp 825-835.

[16] Zeevi, Y., Gertner, I., "The Finite Zak Transform: An Efficient Tool for Image Representation and Analysis", *Journal of Visual Communication and Image Representation*, Vol. 3, pp. 13-23, March 1992.

[17] M. Vetterli, "Filter Banks Allowing Perfect Reconstruction", *Signal Processing*, vol. 10 , pp. 219–244, 1986.

[18] M. Vetterli, D. Le Gall, "Perfect Reconstruction FIR Filter Banks: Some Properties and Factorizations", *IEEE Trans. on Acoust., Speech, and Signal Processing*, vol. 37, pp. 1057–1071, July 1989.

[19] P. P. Vaidyanathan, *Multirate Systems and Filter Banks*, Prentice-Hall, Englewood Cliffs, NJ, 1992

[20] A. J. E. M. Janssen, "The Zak Transform: a Signal Transform for Sampled Time-Continuous Analysis", *Philips J. Res.*, vol. 43, pp. 23–69, 1988.

[21] N.Polyak and W. A. Pearlman, "Filters and Filter Banks for Periodic Signals, the Zak transform and Fast Wavelet Decomposition", IEEE Trans. on Signal Processing, Special Issue on Theory and Applications of Filter Banks and Wavelet Transform, vol. 46, pp. 857-873, April

1998

[22] C. W. Kim and R. Ansari "FIR/IIR Exact Reconstruction Filter Banks with Applications to Subband Coding of Images", Midwest Symposium on Circuits and Systems, July 1991

[23] R. Ansari, S. H. Lee and L. Wu "Subband Image Coding Using IIR Filters", *Proc. Princeton Conf. Info. Sci. and Systems*, pp. 16-21, March 1988

[24] M. J. T. Smith, T. P. Barnwell III, "Exact Reconstruction Techniques for Tree Structured Subband Coders", *IEEE Trans. on Acoust., Speech and Signal Processing*, Vol. ASSP-34, June 1986, pp. 434-441

[25] A. Divakaran and W. A. Pearlman, "Information-Theoretic Performance of Quadrature Mirror Filters", *IEEE Trans. on Information Theory*, vol. 41, no. 6, pp. 2094-2100, Nov. 1995

[26] N. Polyak, *New Wavelet-Based Algorithms for Signal Decomposition and Reconstruction via the Theory of Circular Stationary Vector Sequences and the Zak Transform with Applications to Image Compression*, Ph. D. Thesis, Rensselaer Polytechnic Institute, May 1998.

[27] P. P. Vaidyanathan, "Theory of Optimal Orthonormal Coder", *IEEE Trans. on Signal Processing*, vol. 46, no. 6, pp 1528-1543, June 1998

[28] A. N. Akansu and R. A. Haddad, "Multiresolution Signal Decomposition: Transforms, Subbands and Wavelets", *Academic Press*, 1992

[29] J. Katto and Y. Yasuda, "Performance Evaluation of Subband Coding and Optimization of its Filter Coefficients", *Proc. of SPIE Visual Communications and Image Processing*, Vol. 1605, p. 95-106, Nov. 1991

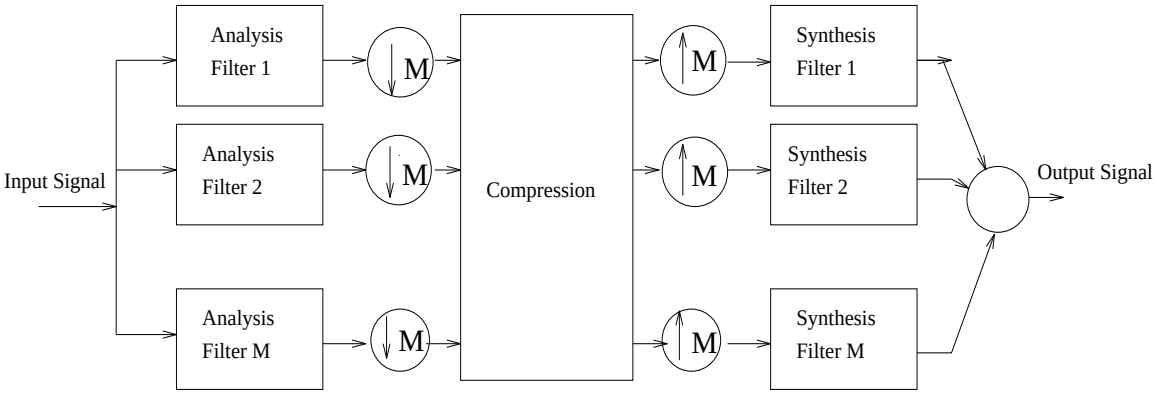

Figure 1: Decomposition and Reconstruction Filter Banks with Compression

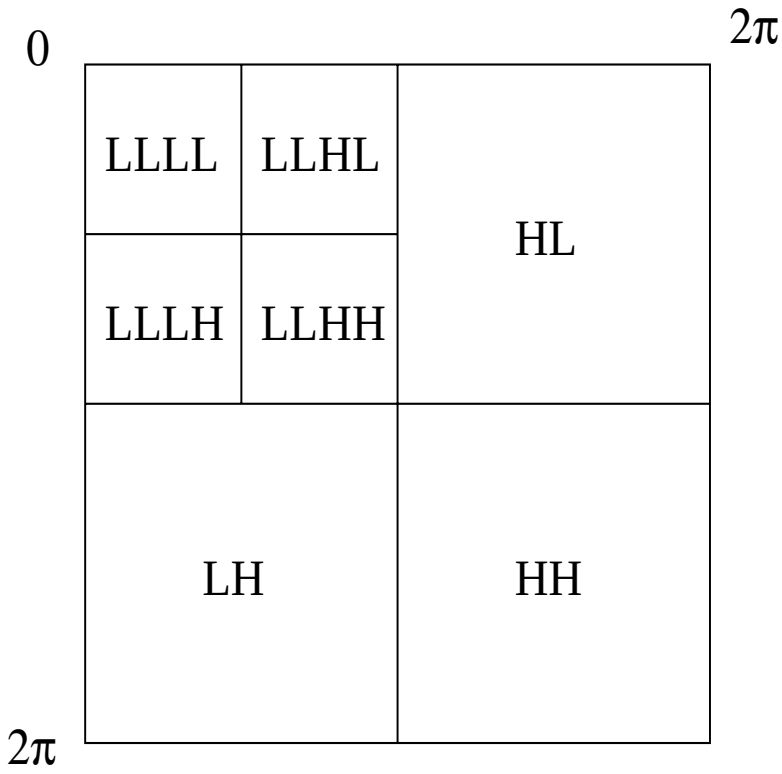

Figure 2: Image Subband Decomposition

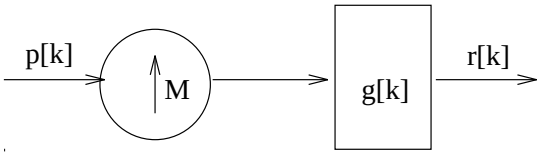

Figure 3: Reconstruction one channel filter bank

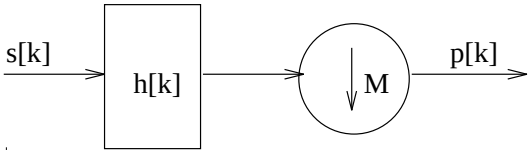

Figure 4: Decomposition one channel filter bank

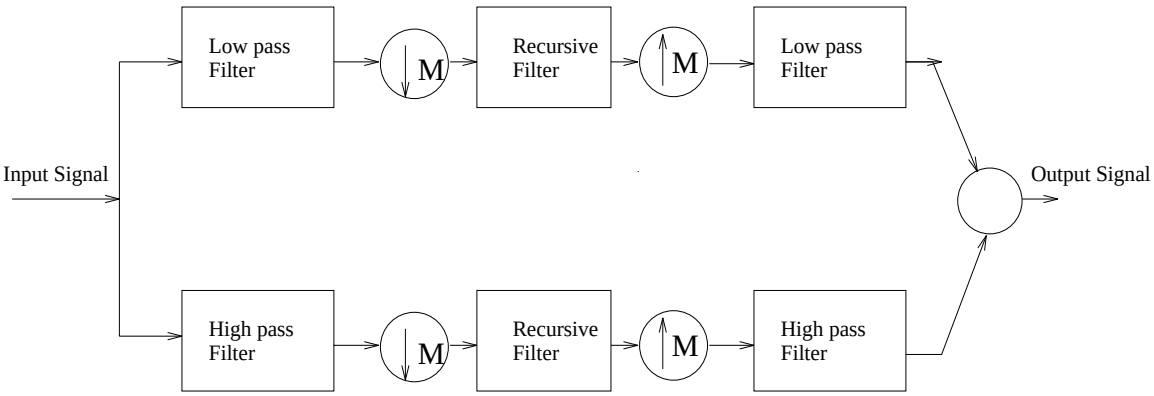

Figure 5: Ideal reconstruction two filter bank with recursive post filters. Compression or any other processing can be performed either before or after the recursive post filters

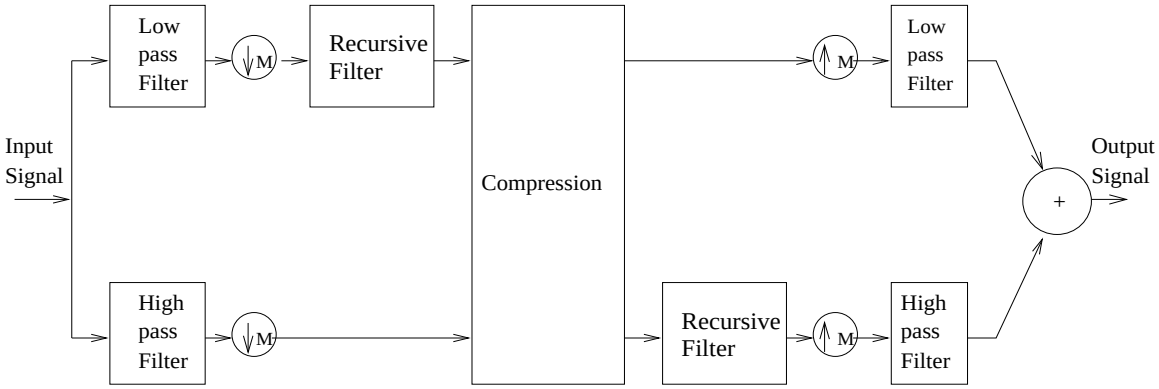

Figure 6: The filter bank with compression used in simulations

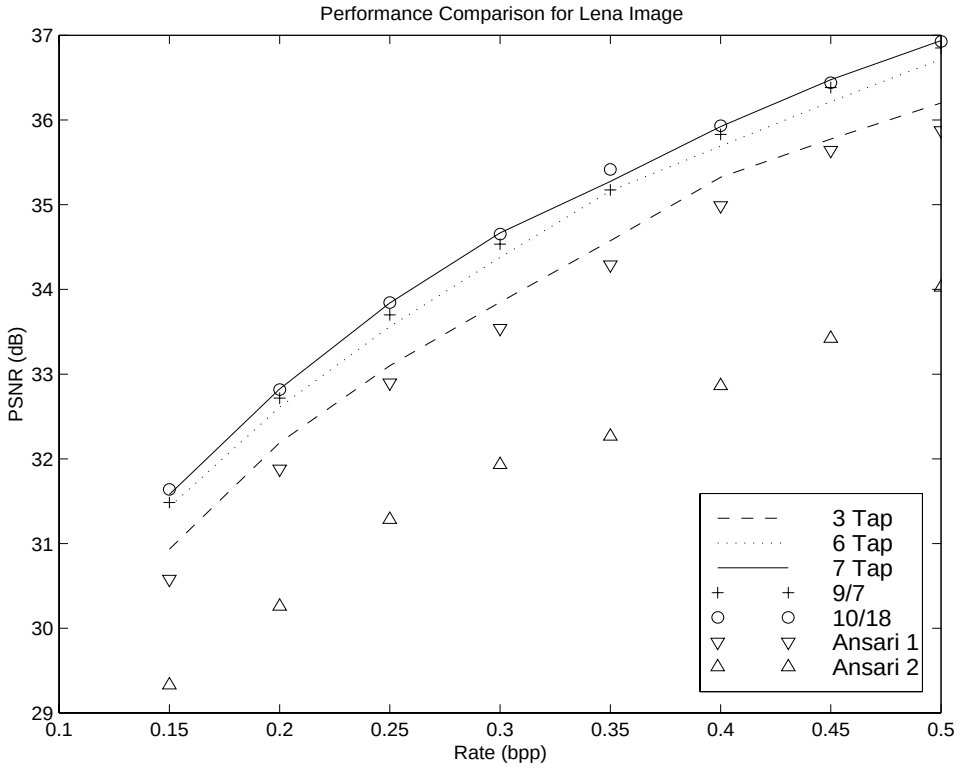

Figure 7: Orthogonal Filters Performance Comparison for Lena Image

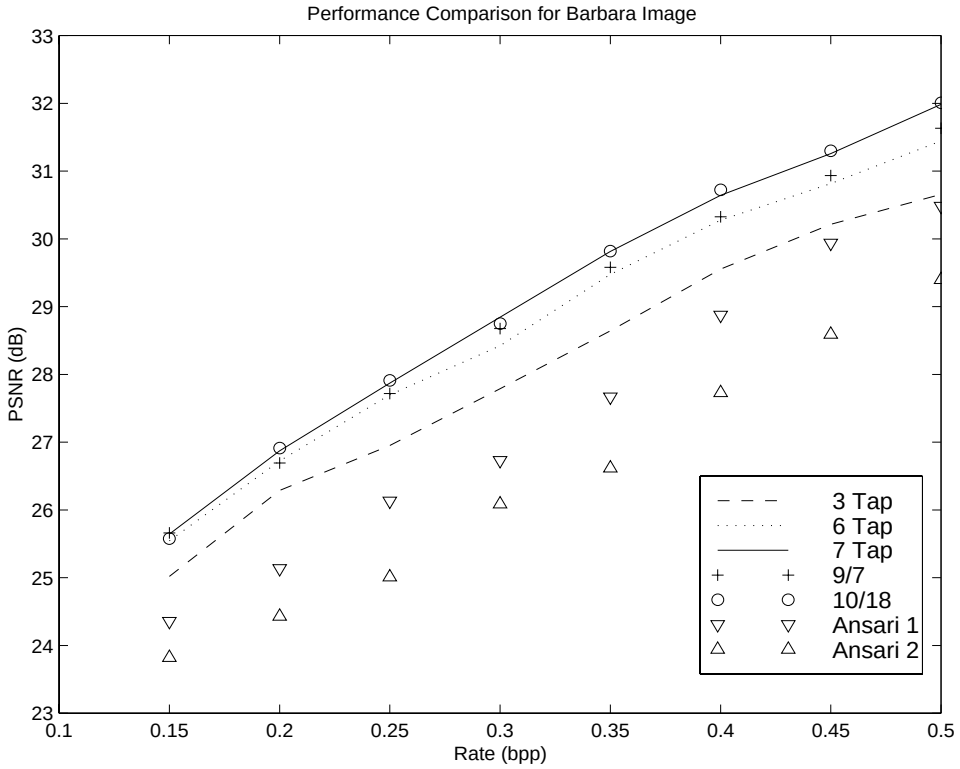

Figure 8: Orthogonal Filters Performance Comparison for Barbara Image

Figure 9: Lena image restored after SPIHT compression at 0.25 bpp rate. From left to right: our 7 tap filter result, 9/7 filter result

Figure 10: From left to right: Lena image restored after SPIHT compression at 0.25 bpp rate, under 10/18 filter, Original Lena image

Figure 11: Barbara image restored after SPIHT compression at 0.25 bpp rate. From left to right: our 7 tap filter result, 9/7 filter result

Figure 12: From left to right: Barbara image restored after SPIHT compression at 0.25 bpp rate, under 10/18 filter, Original Barbara image